Robust 3-component optical fiber accelerometer for seismic monitoring

Dongshan Jiang (蒋东山), Faxiang Zhang (张发祥), Wentao Zhang (张文涛)*,
Feng Li (李　峰), and Fang Li (李　芳)

Optoelectronic System Laboratory, Institute of Semiconductors, Chinese Academy of Science, Beijing 100083, China

*Corresponding author: zhangwt@semi.ac.cn

A robust cantilever-based push–pull 3-component (3-C) optical fiber accelerometer is proposed and experimentally demonstrated. Sensitivity and resonance frequency can be enhanced simultaneously by increasing the number of turns of an optical fiber without increasing the accelerometer size at the mass of a certain value. The calibration results show that axis sensitivity is 45 dB (re: 0 dB = 1 rad/g), with a fluctuation less than 0.9 dB in a frequency bandwidth of 10–450 Hz. The cross sensitivity is approximately 15 dB, with a fluctuation less than 1.2 dB in a frequency bandwidth of 10–450 Hz. The crosstalk reaches up to 30 dB. Fluctuation of the responses of the acceleration sensitivity of different components is less than 0.7 dB over a frequency bandwidth of 10 –450 Hz, which proves the good consistency of the 3-C optical fiber accelerometer. By usingan all-metal structure is expected to improve the reliability of the designed accelerometer for long-term use in harsh environments. These desirable features show that the proposed 3-C optical fiber accelerometer is satisfactory for seismic wave monitoringin oil and gas exploration.

OCIS codes: 060.1155, 060.2370, 280.4788.

doi: 10.3788/COL201311.020602.

An accelerometer is widely used for the detection of vibration signals. Researchers have extensively studied accelerometers in the fields of underwater communication[1], target discrimination[2], oil well logging[3−5], and permanent reservoir monitoring[6−8]. An optical fiber accelerometer is very suitable for hostile environments because of its distinguished advantages, such as its immunity to electromagnetic interference, electrically passive sensing, capability to withstand high temperature and pressure, compared with a conventional electrical accelerometer. A 3-component (3-C) optical fiber accelerometer is often realized by multiplexing three components orthogonally. In Ref. [3], an accelerometer uses compliant material, such as sensing elements. However, more effort has to be exerted to understand that factors that affect the performance of such accelerometers[9]. These factors include the consistency of acceleration sensitivities in different components and the reliability of long-term use, which are important for large-scale optical fiber accelerometer array and sensing networks. Recently, Wang *et al.*[10] revealed the use of cupreous thin-walled annuluses as sensing elements, which broaden the frequency bandwidth and improve the consistency of the responses of different components. However, the acceleration sensitivity of annuluses is only 32.6 dB (re: 0 dB = 1 rad/g), which limits the monitoring of the weak acceleration signal.

In this letter, we report on the design and performance of a robust cantilever-based push–pull 3-C optical fiber accelerometer. The experimental results demonstrate the excellent features of the proposed 3-C optical fiber accelerometer, making it a promising instrument in oil and gas monitoring.

Figure 1 shows the system structure of a 3-C fiber optic accelerometer. This accelerometer comprises a light source, a sensing head, and a unit for signal detecting and processing. The light from the narrow line width fiber laser is split into three beams by an isolator and two couplers. Three beams are launched into the three orthogonal accelerometers by couplers and a cable, respectively. The returned lights are detected and then demodulated by the corresponding detectors and signal processor. Each accelerometer is constructed by a cantilever, a metal mass, two fixed cylinders, and a base. Two sensing optical fibers are wrapped around each of the two fixed cylinders and a metal mass, respectively, to form two arms of an optical fiber Michelson interferometer in a push–pull type. Two Faraday rotation mirrors (FRMs) form the reflecting mirror of each arm of the Michelson interferometer. When the accelerometer is under axial acceleration, the inertia force produced by the metal mass deforms the cantilever, which compresses and extends the two arms of the optical fiber interferometer, and changes the length of the optical fiber. This phenomenon results in a phase shift in the optical fiber interferometer. Acceleration can be extracted by detecting the phase shift. When the accelerometer is under cross acceleration, two face-to-face optical fiber coils have the same deformation. No phase shift is introduced in the optical fiber interferometer. Thus, no signal is detected. Hence, different components of a 3-C optical fiber accelerometer are sensitive only to axial acceleration, resulting in excellent directivity. The length and width of the cantilever are made much larger than the thickness to improve directivity, making the cantilever prone to bending only in the axis direction. This step enhances the directivity of the accelerometer.

Generally, analysis of a 3-C optical fiber accelerometer is based on a single cantilever loaded with a mass. Figure 2 shows the simplified deformation of an optical fiber accelerometer in the non-inertial system for the acceleration of $Ae^{-i\omega t}$, where A and ω are the magnitude
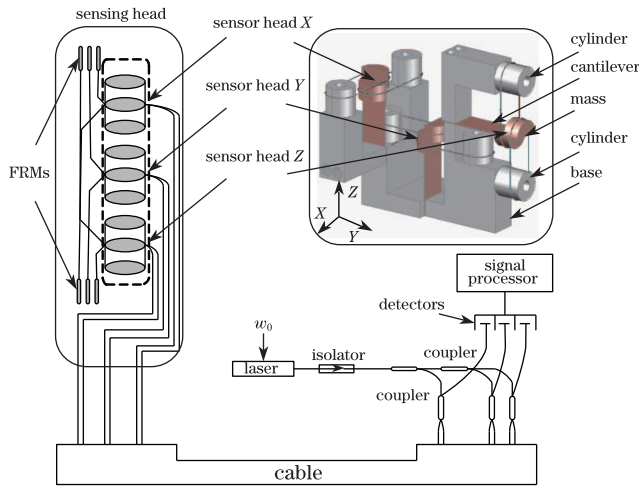
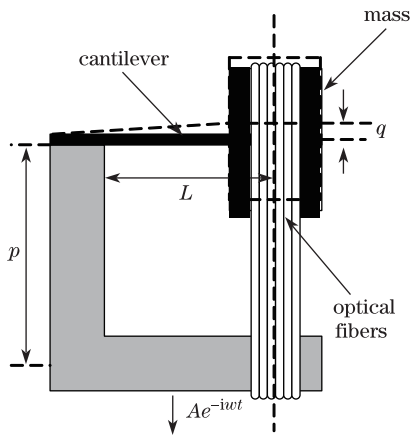Fig. 1. System structure of 3-C optical fiber accelerometer.

Fig. 2. Schematic of deformation of optical fiber accelerometer in non-inertial system.

and angular frequency of acceleration. The other arm of the optical fiber Michelson interferometer is neglected in Fig. 2. The kinetic and potential energy of the system can be expressed as

$$T = \frac{1}{2}m\dot{q}^2, \tag{1}$$

$$V = V_{\rm f} + V_{\rm b}, \tag{2}$$

where $V_{\rm f}$ and $V_{\rm b}$ are the potential energies of the optical fiber and the cantilever, respectively; T is kinetic energy of mass; q is maximum deflection of the cantilever.

Assuming that optical fiber is elastic model, $V_{\rm f}$ is given by

$$V_{\rm f} = \frac{4NA_{\rm f}E_{\rm f}}{l}q^2, \tag{3}$$

where N, $A_{\rm f}$, and $E_{\rm f}$ are the number of turns, cross-sectional area, and Young's modulus of the optical fiber, respectively; $l = 2\pi r + 2p$ is the length of each coil optical fiber; r is the same radius of the metal mass and fixed cylinder; p is the length between the cantilever and the middle part of the fixed cylinder.

The schematic of the cantilever deformation is shown in Fig. 2. By using a concentrated load of cantilever

deformation model[11], $V_{\rm b}$ is given as

$$V_{\rm b} = \frac{Ebh^3q^2}{8L^3}, \tag{4}$$

where L, b, h, and E are the length, width, thickness, and Young's modulusof the cantilever, respectively.

T and V are substituted into the Lagrange equation. The kinetic equation can then be described as

$$m\ddot{q} + \left(\frac{8NA_{\rm f}E_{\rm f}}{l} + \frac{Ebh^3}{4L^3}\right)q = mAe^{-i\omega t}. \tag{5}$$

By solving Eq. (5), we obtain

$$q = q_0 e^{-i\omega t} = \frac{mA}{-m\omega^2 + \left(\frac{8NA_{\rm f}E_{\rm f}}{l} + \frac{Ebh^3}{4L^3}\right)}e^{-i\omega t}. \tag{6}$$

The phase delay for the length change of two arms of the optical fiber Michelson interferometer is

$$\Delta\varphi = 4(1 - p_{\rm e})nkN\Delta l, \tag{7}$$

where $p_{\rm e} = 0.22$ is the elastic-optic coefficient of the optical fiber, n is the refractive index of the optical fiber core, k is the wavenumber of the optical signal, and $\Delta l = 2q_0$ is the variation of each coil optical fiber.

Based on Eqs. (6) and (7), the acceleration sensitivity of the optical fiber accelerometer can be expressed by

$$S_{\rm a} = \frac{S_0}{1 - \frac{f^2}{f_0^2}}, \tag{8}$$

where S_0 and f_0 are the acceleration sensitivity and the resonance frequency of the optical fiberaccelerometer, respectively.

From Eq. (8), we have

$$S_0 = \frac{0.78 \cdot N \cdot 8n \cdot k \cdot m}{\frac{8NA_{\rm f}E_{\rm f}}{l} + \frac{Ebh^3}{4L^3}}, \tag{9a}$$

$$f_0 = \frac{1}{2\pi}\sqrt{\frac{1}{m}\left(\frac{8NA_{\rm f}E_{\rm f}}{l} + \frac{Ebh^3}{4L^3}\right)}. \tag{9b}$$

According to Eq. (9a), when the number of turns of an optical fiber reaches ∞, the acceleration sensitivity reaches a maximum value. The theoretical maximum value of the acceleration sensitivity can be represented by

$$S_0 = \frac{0.78 \cdot n \cdot k \cdot m \cdot l}{A_{\rm f}E_{\rm f}}. \tag{10}$$

Acceleration sensitivity and resonance frequency exist in the relationship of mutual constraint; acceleration sensitivity improves by increasing the mass at the expense of resonance frequency, and vice versa[9]. However, based on Eqs. (9a) and (9b), the acceleration sensitivity and resonance frequency can be easily enhanced by increasing the number of turns of an optical fiber when accelerometer size does not increase at the mass of a certain value. Figure 3 shows the relationship of both acceleration sensitivity and resonance frequency with number of turns of the optical fiber; the other parameters are given in Table 1.

Figure 3 shows that resonance frequency can be improved through increasing number of turns of the optical fiber, broadening the frequency bandwidth when acceleration sensitivity reaches a maximum value. In samples,

Table 1. Parameters of Optical Fiber Accelerometer

Parameter	Value
n	1.456
m (g)	32
k (m^{-1})	4×10^6
b (mm)	16
h (mm)	0.5
L (mm)	33
l (mm)	123
r (mm)	9
p (mm)	33
E_{f} (Gpa)	72
E (Gpa)	102
A_{f} (mm^2)	0.0123
λ (mm)	1550
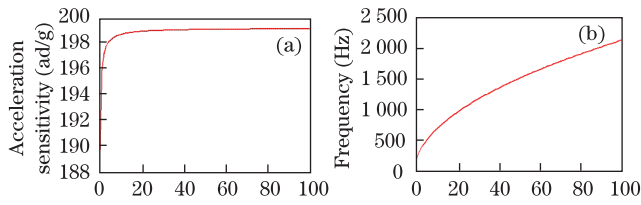
Fig. 3. Relationships between (a) acceleration sensitivity and (b) resonance frequency and number of turns.
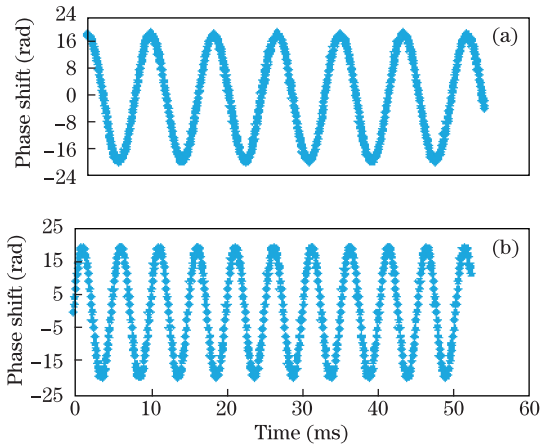

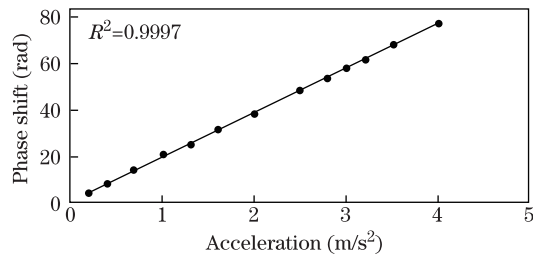Fig. 4. Time domain trace with acceleration of 0.1 g at (a) 100 and (b) 200 Hz.

Fig. 5. Response of phase shift versus acceleration.

N=20. The other parameters are given in Table 1. The theoretical acceleration sensitivity is approximately 46 dB and the resonance frequency is 956 Hz.

A series of acceleration measurements verify the dynamic characteristics of the 3-C optical fiberaccelerometer. Considering that it is difficult to find an acceleration source that can generate acceleration in the arbitrary direction, we change the installation of the accelerometer to simulate acceleration in different directions for the experiments. A standard piezoelectric accelerometer (BK4371) is attached below the accelerometer to calibrate the acceleration of each component. A precision-shaking table (BKV650) provides as eries of sine excitations with tunable frequency as input signal. The output of the accelerometer is demodulated by aphase interrogator with a resolution of 10^{-5} rad and a sampling frequency of 10 kHz.

During the experiment, the input acceleration signal remains at 0.1 g. The time domain trace is shown in Fig. 4 with the frequencies of 100 and 200 Hz for accelerometer z, which is shown in Fig. 1. Good response is observed. The experimental results show that the accelerometer is capable of monitoring acceleration.

For an ideal optical fiber accelerometer, the phase shift and acceleration should maintain linear relationship in the measurement range and frequency bandwidth. In the experiment, the amplitude of acceleration varies from 0.2 to 4 m/s^2, with a constant frequency of 100 Hz for accelerometer z in Fig. 1. Linear fitting results in Fig. 5 show good linearity between the phase shift and acceleration. The correlation coefficient R is 0.9998.

Axial and cross acceleration sensitivities are crucial characteristics of an optical fiberaccelerometer. Figure 6 shows the frequency response of the axial and cross sensitivity of accelerometer z in Fig. 1, respectively. The axial sensitivity is approximately 45 dB, with a fluctuation less than 0.9 dB in a frequency bandwidth of 10–450 Hz. The resonance frequency is approximately 900 Hz. Both axial sensitivity and resonance frequency are in good agreement with the theoretical analysis presented in Eqs. (9a) and (9b). The cross sensitivity is approximately 15 dB, with a fluctuation less than 1.2 dB in a frequency bandwidth of 10–450 Hz. The crosstalk reaches up to 30 dB. These results indicate that the designed accelerometer is sensitive to axial acceleration, but not to cross acceleration.

In seismic monitoring, the consistency of the acceleration sensitivity of a 3-C optical fiber accelerometer is important in large-scale optical fiber accelerometer arrays. Figure 7 shows the measured frequency response of the acceleration sensitivity
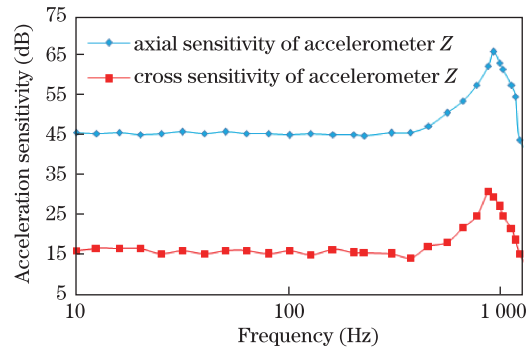

Fig. 6. Frequency response of axial and cross acceleration sensitivity of accelerometer.
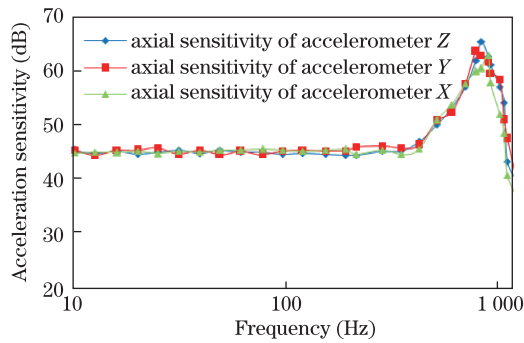
Fig. 7. Frequency response of acceleration sensitivity of 3-C optical fiber accelerometer in three orthogonal directions.

of each component in three orthogonal directions. The responses of the acceleration sensitivity of the different components fluctuate at less than 0.7 dB over a frequency bandwidth of 10–450 Hz, which proves good consistency of the 3-C optical fiberaccelerometer. The measured results indicate that the proposed 3-C optical fiber accelerometer is promising in building a large-scale optical fiberaccelerometer array for future application.

In conclusion, a robust cantilever-based push–pull 3-C optical fiber accelerometer is proposed and studied. An all-metal structureis expected to improve the reliability of the accelerometer for long-term use in harsh environments. Sensitivity and resonance frequency can be enhanced simultaneously by increasing number of turns of the optical fiber without increasing accelerometer size at them ass of a certain value. The accelerometer's superiorities in sensitivity, crosstalk, frequency bandwidth, and consistency manifest in the calibration results. Axial sensitivity is 45 dB, with a fluctuation less than 0.9 dB in a frequency bandwidth of 10–450 Hz. The resonance frequency is approximately 900 Hz. Cross sensitivity is

approximately 15 dB, with a fluctuation less than 1.2 dB in a frequency bandwidth of 10–450 Hz. The crosstalk reaches up to 30 dB. The responses of the acceleration sensitivity of different components fluctuate by less than 0.7 dB over a frequency bandwidth of 10–450 Hz, which proves good consistency for the 3-C optical fiber accelerometer. These results show that the proposed 3-C optical fiber accelerometer is a good candidate for seismic wave monitoring system in oil and gas explorations.

References

1. A. Song, A. Abdi, M. Badiey, and P. Hursky, IEEE J. Ocean. Eng. **36,** 454 (2011).
2. J. A. Clark and G. Tarasek, in *Proceedings of OCEANS2006* 1 (2006).
3. N. Zeng, C. Shi, M. Zhang, L. Wang, Y. Liao, and S. Lai, Opt. Commun. **234,** 153 (2004).
4. B. E. Hornby, F. X. Bostick, B. A. Williams, K. A. Lewis, and P. G. Garossino, Geophysics **70,** E11 (2005).
5. Y. Weng, X. Qiao, Z. Feng, M. Hu, J. Zhang, and Y. Yang, Chin. Opt. Lett. **9,** 100604 (2011).
6. R. J. Brown, Geophysics **75,** Q11 (2010).
7. N. C. Rowe, Proc. SPIE **7693,** 76930T (2010).
8. J. T. Kringlebotn, H. Nakstad, and M. Eriksrud, Proc. SPIE **7503,** 75037U (2009).
9. J. M. D. Freitas, Meas. Sci. Technol. **22,** 8 (2011).
10. J. Wang, H. Luo, Z. Meng, and Y. Hu, J. Lightwave Technol. **30,** 1178 (2012).
11. H. Liu, *Mechanics of Materials* (Higher Education Press, Bei Jing, 2004).